



HAL
open science

Redox-Active Glyconanoparticles as Electron Shuttles for Mediated Electron Transfer with Bilirubin Oxidase in Solution

Andrew Gross, Xiaohong Chen, Fabien Giroud, Christophe Travelet,
Redouane Borsali, Serge Cosnier

► **To cite this version:**

Andrew Gross, Xiaohong Chen, Fabien Giroud, Christophe Travelet, Redouane Borsali, et al.. Redox-Active Glyconanoparticles as Electron Shuttles for Mediated Electron Transfer with Bilirubin Oxidase in Solution. *Journal of the American Chemical Society*, 2017, 139 (45), pp.16076 - 16079. 10.1021/jacs.7b09442 . hal-01649354

HAL Id: hal-01649354

<https://hal.science/hal-01649354>

Submitted on 19 Nov 2020

HAL is a multi-disciplinary open access archive for the deposit and dissemination of scientific research documents, whether they are published or not. The documents may come from teaching and research institutions in France or abroad, or from public or private research centers.

L'archive ouverte pluridisciplinaire **HAL**, est destinée au dépôt et à la diffusion de documents scientifiques de niveau recherche, publiés ou non, émanant des établissements d'enseignement et de recherche français ou étrangers, des laboratoires publics ou privés.


1 Redox-Active Glyconanoparticles as Electron Shuttles for Mediated 2 Electron Transfer with Bilirubin Oxidase in Solution

3 Andrew J. Gross,^{†,‡,Ⓛ} Xiaohong Chen,^{‡,Ⓛ} Fabien Giroud,^{‡,Ⓛ} Christophe Travelet,^{†,§}
4 Redouane Borsali,^{*,†,§,Ⓛ} and Serge Cosnier^{*,‡}

5 [‡]Department of Molecular Chemistry, CNRS UMR 5250, DCM, Université Grenoble Alpes, 38000 Grenoble, France

6 [†]CERMAV, Université Grenoble Alpes, 38000 Grenoble, France

7 [§]CNRS UPR 5301, CERMAV, 38000 Grenoble, France

8  Supporting Information

9 **ABSTRACT:** We demonstrate self-assembly, character-
10 ization and bioelectrocatalysis of redox-active cyclodextrin-
11 coated nanoparticles. The nanoparticles with host–guest
12 functionality are easy to assemble and permit entrapment
13 of hydrophobic redox molecules in aqueous solution. Bis-
14 pyrene-ABTS encapsulated nanoparticles were investigated
15 electrochemically and spectroscopically. Their use as
16 electron shuttles is demonstrated via an intraelectron
17 transfer chain between neighboring redox units of
18 clustered particles ($D_{h,DLS} = 195$ nm) and the mono-
19 and trinuclear Cu sites of bilirubin oxidases. Enhanced
20 current densities for mediated O_2 reduction are observed
21 with the redox nanoparticle system compared to
22 equivalent bioelectrode cells with dissolved mediator.
23 Improved catalytic stability over 2 days was also observed
24 with the redox nanoparticles, highlighting a stabilizing
25 effect of the polymeric architecture. Bioinspired nano-
26 particles as mediators for bioelectrocatalysis promises to be
27 valuable for future biofuel cells and biosensors.

28 **E**lectron transfer (ET) reactions are vital in biological
29 systems including metabolic pathways and photosyn-
30 thesis.¹ In nature, many ET processes involve redox proteins
31 that rely on intramolecular electron transfer and long-range
32 electron transport between enzymes. The high efficiency and
33 specificity of nature's biocatalysts has driven the development
34 of biomimetic enzyme–electrode interfaces for applications such
35 as energy conversion and biosensing.² Biofuel cells are
36 emerging devices for converting chemical energy into electrical
37 energy which ideally exploit fast and efficient ET between
38 electrodes and enzymes.³ In most cases, such electron transfer
39 reactions are hampered due to the insulating globular structure
40 of the protein matrix surrounding the enzyme's active site.
41 Improvements in the electrical wiring of enzymes and the
42 stability of enzyme–electrode interfaces are required to address
43 limitations of biofuel cells including limited operational stability
44 and low power output.

45 Direct electron transfer (DET) over short distances (≤ 1.5
46 nm) between the redox center(s) of enzymes and electrodes
47 has been achieved for a limited number of enzymes including
48 multicopper oxidases (MCOs). MCOs are of great interest for
49 the reduction of O_2 at the cathode in biofuel cells.^{4,5} Mediated

electron transfer (MET) is an alternative to DET that enables
50 ET with a wide range of enzymes. For MET, redox polymers
51 and redox molecules are employed to shuttle electrons to and
52 from the enzyme's active site.^{6,7} This can reduce the kinetic
53 hindrance of interfacial ET but commonly at the expense of a
54 high overpotential. Use of a mediator is attractive, but complex
55 synthesis, chemical stability and leaching of the mediator *in vivo*
56 and *ex vivo* are major concerns. An approach to address these
57 limitations has been to use carbon or metal nanoparticles
58 (NPs).
59

60 Early work has described the use of gold NPs functionalized
61 with enzyme cofactor for high catalytic turnover of glucose via
62 modified apo-glucose oxidase (GOx)⁸ and apo-glucose
63 dehydrogenase.⁹ More recently, gold NPs have been elegantly
64 bonded to GOx and MCO enzymes to facilitate enzyme wiring
65 with the electrode.^{10,11} While these examples highlight
66 improved enzyme wiring via electronic bridging, multistep
67 synthesis and protein engineering are necessary. Alternatively,
68 carbon and metal NPs directly immobilized on electrode
69 surfaces create high area meso- and nanostructured interfaces
70 for DET via oriented immobilization and enzyme trapping.^{12,13}
71 Surface immobilization of catalytic components is the classic
72 approach for biofuel cell construction. Immobilization is
73 considered effective for electrode stabilization. Nevertheless,
74 desorption, limiting surface coverages and enzyme activity loss
75 (for example, due to conformational changes) are constraining
76 factors.^{14,15}

77 Here, we further extend the use of MET between electrodes
78 and enzymes to a strategy which uses mediator-containing
79 sugar-coated nanoparticles in solution. To the best of our
80 knowledge, no polymeric nanoparticle system has been
81 explored either for ET with enzymes or for bioelectrocatalysis.
82 In addition, we move away from the mainstream use of
83 immobilized biocatalytic components and instead explore their
84 use only in solution. This unconventional approach in
85 particular opens up the possibility for (i) higher amounts of
86 enzyme and mediator, (ii) improved enzymatic activity and (iii)
87 the possibility to refuel electrode compartments for prolonged
88 fuel cell performance. The cyclodextrin-based NPs are
89 envisaged here for solution-based biofuel cells and flow-through

Received: September 8, 2017

Published: October 31, 2017



90 biosensors but could also be harnessed for applications
91 including light harvesting.¹⁶

92 The encapsulated nanoparticles were prepared by self-
93 assembly of an amphiphilic β -cyclodextrin modified polystyrene
94 polymer (PSCD) (Figure 1A). The PSCD polymer was

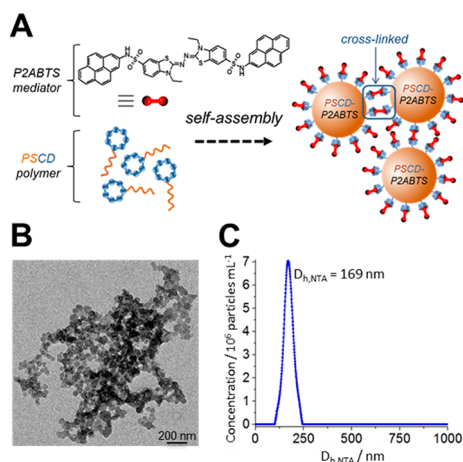


Figure 1. (A) Schematic representation of the self-assembly of bis-pyrene-ABTS encapsulated glyconanoparticles. (B) TEM imaging and (C) hydrodynamic diameter distribution by NTA of PSCD-P2ABTS_{NP}.

95 synthesized according to a convenient protocol via click
96 chemistry of functionalized cyclodextrin and polystyrene blocks
97 in high yield.¹⁷ Self-assembly of PSCD was explored in the
98 absence and presence of bis-pyrene-ABTS (2,2'-Azino-bis(3-
99 ethylbenzothiazoline-6-sulfonic acid)) via nanoprecipitation in
100 a large excess of water (see Supporting Information).

101 The possibility to spontaneously self-assemble nanoparticles
102 from β -cyclodextrin modified polystyrene solutions was first
103 confirmed by transmission electron microscopy (TEM) and
104 nanoparticle tracking analysis (NTA). TEM imaging of the bis-
105 pyrene-ABTS nanoparticles (PSCD-P2ABTS_{NP}) revealed ag-
106 gregated clusters composed of individual nanoparticles with an
107 average diameter of 51 ± 18 nm (Figure 1B). NTA analysis
108 revealed direct evidence for NPs undergoing Brownian motion
109 with $D_{h,NTA} = 169$ and 74 nm for the PSCD-P2ABTS_{NP}
110 nanoparticles and unmodified nanoparticles (PSCD_{NP}),
111 respectively (Figure 1C and S1). The difference between self-
112 assembly performed in the absence and presence of bis-pyrene-
113 ABTS is consistent with the incorporation of guest molecules.
114 The clusters can form in solution with bis-pyrene-ABTS
115 molecules functioning as molecular bridges where each pyrene
116 functionality forms a 1:1 inclusion complex with a β -
117 cyclodextrin cavity present in the outer layer of individual
118 nanoparticles.¹⁸ Nonspecific aggregation must also be consid-
119 ered and likely contributes to the self-assembly of the clusters.

120 Dynamic light scattering (DLS) experiments were performed
121 to examine the PSCD-P2ABTS_{NP} nanoparticles in more detail
122 (Figure 2A). The relaxation time distribution plot, correspond-
123 ing to a mass-weighted distribution, reveals the presence of two
124 particle sizes with $D_{h,DLS} = 195$ and 1800 nm according to
125 Equation S1. The smaller population is complementary to that
126 obtained by NTA. The larger population confirms the presence
127 of large agglomerations in the suspension but their presence is
128 very small in number terms. Assuming that the particles behave
129 like a hard sphere in water and have the same density, the

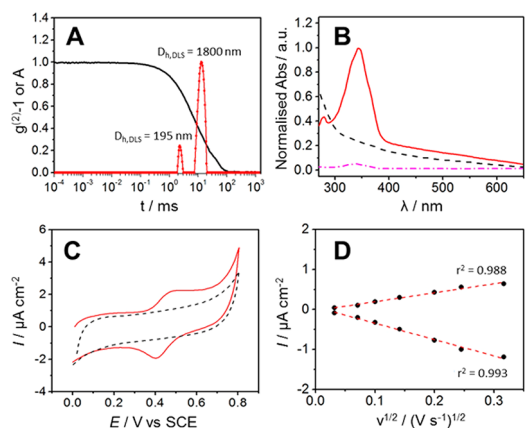


Figure 2. (A) DLS autocorrelation function ($g^{(2)}-1$) measured at 90° and relaxation time distribution of PSCD-P2ABTS_{NP}. (B) UV-visible spectra for (red —) PSCD-P2ABTS_{NP}, (—) PSCD_{NP} and (---) H₂O-P2ABTS. (C) CVs at glassy carbon of as-prepared (red —) PSCD-P2ABTS_{NP} and (---) PSCD_{NP} at 100 mV s^{-1} . (D) Corresponding plots of peak current vs the square root of the scan rate for PSCD-P2ABTS_{NP}.

130 estimated number of the smaller objects with $D_{h,DLS} = 195$ nm
131 is 97.5% according to Equation S2.

132 The feasibility to encapsulate bis-pyrene-ABTS during
133 nanoparticle self-assembly was established by UV-visible
134 spectroscopy (Figure 2B). Three suspensions were inves-
135 tigated: as-prepared PSCD_{NP} and PSCD-P2ABTS_{NP}, and
136 saturated bis-pyrene-ABTS (H₂O-P2ABTS) in 0.1 M phos-
137 phosphate buffer (PB). The absorption spectrum for PSCD_{NP} shows
138 background absorbance due to the polymer and no well-defined
139 peaks. In contrast, PSCD-P2ABTS_{NP} and H₂O-P2ABTS exhibit
140 a single well-defined absorption peak at $\lambda_{\text{max}} = 344$ and 340 nm,
141 respectively, confirming the presence of the ABTS functionality.
142 The absorption is markedly enhanced for PSCD-P2ABTS_{NP}
143 compared to the saturated H₂O-P2ABTS solution, consistent
144 with a dramatic improvement in solubility for bis-pyrene-ABTS
145 via the polymeric architecture. The concentration of bis-pyrene-
146 ABTS in PSCD-P2ABTS_{NP} was estimated to be $6.5 \mu\text{M}$ based
147 on linear calibration curves obtained for both ABTS and
148 ABTS^{•-} solutions (Figure S2).

149 The electroactivity of as-prepared PSCD-P2ABTS_{NP} and
150 PSCD_{NP} nanoparticle solutions was investigated at a glassy
151 carbon electrode (GC) without additional supporting electro-
152 lyte. Figure 2C shows cyclic voltammograms (CVs) recorded at
153 100 mV s^{-1} of the redox encapsulated and control nano-
154 particles. The CVs clearly show a chemically reversible redox
155 couple at $E_{1/2} = 0.46$ V corresponding to the one electron
156 oxidation of ABTS²⁻ to ABTS^{•-} for PSCD-P2ABTS_{NP}. No
157 redox signal is observed for PSCD_{NP} in the absence of bis-
158 pyrene-ABTS. The redox functionalities are therefore clearly
159 present and accessible. The plots in Figures 2D and S3 show
160 that the peak currents for the oxidation and reduction processes
161 are proportional to the square root of the scan rate, as expected
162 for diffusion-controlled behavior. Poor fitting was observed for
163 the peak current vs scan rate over a wide scan rate range,
164 discounting the presence of adsorbed electroactive species.
165 Furthermore, after recording several CV cycles in PSCD-
166 P2ABTS_{NP} solution, no evidence for adsorbed electroactive
167 NPs was observed at a GC electrode in PB (Figure S4).
168 Although this data does not reveal evidence for NP adsorption,
169 the possibility of dynamic adsorption/desorption during

170 potential cycling cannot be entirely ruled out. Repeated
171 potential cycling of PSCD-P2ABTS_{NP} showed good stability
172 with little change in the electrochemical redox activity after 10
173 cycles (Figure S5). The electrochemical stability provides
174 further evidence for the stable entrapment of bis-pyrene-ABTS
175 as well as the oxidized radical form in the nanoparticles.

176 Next the catalytic activity of the PSCD-P2ABTS_{NP} nano-
177 particles for the 4-electron 4-proton reduction of O₂ to water
178 with bilirubin oxidase (BOx from *Myrothecium verrucaria*, 68
179 kDa) was investigated. This enzyme offers high enzymatic
180 activity, stability at neutral pH and stability toward chloride
181 ions.¹⁹ Figure 3 shows CVs that demonstrate bioelectrocatalytic

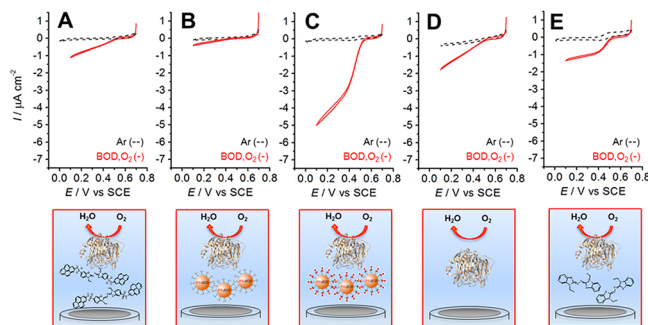


Figure 3. CVs recorded at GC at 5 mV s⁻¹ (pH = 5.6) with (--) argon saturation and (red -) O₂ saturation with BOx for (A) saturated bis-pyrene-ABTS in PB, (B) as-prepared PSCD_{NP} (pH = 5.9), (C) as-prepared PSCD-P2ABTS_{NP}, (D) BOx only and (E) ABTS in PB. [BOx] = 3.5 μmol L⁻¹ and [mediator] = 6.5 μmol L⁻¹ (<6.5 μmol L⁻¹ for saturated bis-pyrene-ABTS).

182 O₂ reduction at GC with 3.5 μmol L⁻¹ BOx in quiescent
183 oxygen saturated solution ([O₂] ~ 1.1 mmol L⁻¹). A summary
184 of the catalytic parameters are displayed in Table S1. For all
185 cases, the limiting catalytic currents were obtained from CVs at
186 0.1 V vs SCE. The biocathodes prepared with the dissolved
187 mediators, bis-pyrene-ABTS and ABTS, exhibited maximum
188 current densities for O₂ reduction of -0.67 ± 0.15 μA cm⁻²
189 (Figure 3A) and -1.20 ± 0.03 μA cm⁻² (Figure 3E),
190 respectively. The smaller current observed with bis-pyrene-
191 ABTS is consistent with its very poor solubility. For the
192 biocathode without NPs or dissolved mediator, a limiting
193 current of 1.39 ± 0.46 μA cm⁻² was obtained (Figure 3D). For
194 this case, effective DET is clearly observed between GC and
195 BOx in solution. Quasi-steady-state (sigmoidal) voltammo-
196 grams are obtained for the PSCD-P2ABTS_{NP} biocathode,
197 which exhibits a comparably remarkable current density of
198 -3.97 ± 0.86 μA cm⁻² (Figure 3C). For the control PSCD_{NP}
199 nanoparticles, very low current densities were observed due to
200 the insulating polymeric structure blocking ET between the
201 enzyme and the electrode (Figure 3B). PSCD-P2ABTS_{NP}
202 solutions prepared at different concentrations (with D_{h,DLS}
203 between 190 and 390 nm) demonstrated a linear dependence
204 of catalytic current on mediator concentration and also revealed
205 a catalytic improvement with the NPs compared to dissolved
206 ABTS (Figure S6 and S7)

207 The enhancement in catalytic current observed for PSCD-
208 P2ABTS_{NP} is consistent with an efficient intramolecular transfer
209 chain between neighboring ABTS redox units of clustered
210 particles and the mono- and trinuclear Cu sites of enzymes in
211 solution, as represented in Figure 4A. The redox conduction
212 observed for bis-pyrene-ABTS nanoparticles at GC is explained

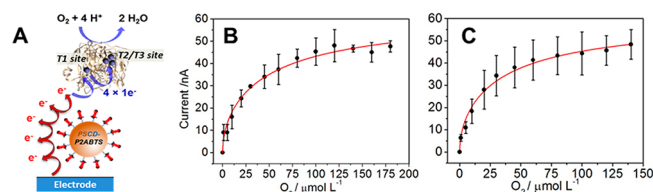


Figure 4. (A) Schematic representation of the intramolecular transfer chain between redox nanoparticles and BOx. (B, C) Plot of limiting current as a function of substrate concentration with line of best fit to Equation S6 for (B) ABTS and (C) P2ABTS_{NP} solutions. [BOx] = 10 nmol L⁻¹ and [med] = 6.5 μmol L⁻¹. Current measured from amperograms at 0.2 V vs SCE.

213 by the phenomena of electron hopping widely reported for
214 redox polymers,²⁰ where electron transfer proceeds by
215 sequential self-exchange steps between adjacent redox groups
216 within, between and on the surface of individual NPs. Mediated
217 electron transfer was also observed for visibly aggregated
218 PSCD-P2ABTS_{NP} in solution, confirming the ability of the
219 redox particles to accept and transfer electrons over substantial
220 distances (Figure S8). The source of catalytic enhancement for
221 the NPs is in part attributed to free rotation of the particles on
222 the time scale of the experiment which allows many redox sites
223 at the NP surface to access enzymatic active sites close to the
224 electrode, enabling many catalytic events. Similar rotation
225 enhancement effects are known with redox dendrimers.²¹
226 Effective redox hopping across and around the redox NPs also
227 allows many "active" mediators, therefore facilitating many
228 enzymes to be connected.

The mediated BOx-catalyzed bioelectrocatalytic reduction of
229 O₂ is considered to follow a ping-pong bi-bi mechanism with a
230 two substrate reaction.⁴ Next, kinetic parameters for PSCD-
231 P2ABTS_{NP} and ABTS were determined from the catalytic
232 current as a function of the substrate (O₂) concentration. This
233 approach permits extraction of the Michaelis constant (K_M)
234 and k_{cat} according to Equation S6, as described by Bartlett and
235 co-workers for mediated homogeneous bioelectrocatalysis via
236 ping-pong enzyme kinetics.²² Figure 4B and 4C shows the
237 calibration plots and nonlinear best fit for the BOx-oxygen
238 reaction with the ABTS and P2ABTS_{NP} mediator solutions
239 containing 10 nmol L⁻¹ BOx, respectively. From amperograms
240 recorded at 0.2 V vs SCE in triplicate, the estimated k_{cat} and K_M
241 values are 142 ± 15 s⁻¹ and 77 ± 15 μmol L⁻¹ for the PSCD-
242 P2ABTS_{NP} mediator and 200 ± 25 s⁻¹ and 107 ± 25 μmol L⁻¹
243 for the ABTS mediator. The different kinetic values suggest that
244 the BOx has a higher affinity for oxygen in the presence of the
245 NPs compared to the dissolved ABTS mediator, although with
246 a slower turnover rate. The values obtained are of the same
247 order reported for MCO enzymes for O₂ reduction in solution
248 including 118 ± 10 s⁻¹ for Tvlaccase/ABTS,²³ and 57 s⁻¹²⁴ and
249 230 s⁻¹¹⁵ for MvBOx/ABTS. The K_M values fall in the general
250 range of 10 to 500 μmol L⁻¹ found in the literature. Crucially,
251 these results confirm that the NPs serve as effective electron
252 relays.

A preliminary assessment of short-term biocathode stability
254 was performed. Amperometric currents were monitored in
255 oxygen-purged solution at 0.2 V vs SCE for periods of 1800 s
256 on 2 days (Figure S9 and Table S2). The catalytic currents were
257 stable during 1800 s for PSCD-P2ABTS_{NP}, ABTS and BOx
258 solutions with 3.5 μmol L⁻¹ BOx. After storage at room
259 temperature overnight, the operational stability during a further
260 1800s remained relatively stable (current fluctuation <10%).
261

262 However, the current densities were drastically lower in all
263 three cases. The percentage of current remaining after 3600 s
264 (2×1800 s) operation and 24 h storage is 67%, 25% and 37%
265 for the PSCD-P2ABTS_{NP}, ABTS and BOx only biocathodes,
266 respectively. After a further 24 h and a total operation time of
267 5400 s, 33% of the initial current remained for the PSCD-
268 P2ABTS_{NP} biocathode. The current density was therefore still
269 higher for the nanoparticle biocathode after 2 days than for the
270 ABTS and BOx after only 1 day. The homogeneous ABTS/
271 BOx solution with MET is therefore extremely unstable. The
272 BOx solution with DET is slightly better but still very poor.
273 Remarkably, a major improvement in biocathode stability was
274 observed using the redox NPs. The improved stability is, at
275 least in part, attributed to the NP architecture stabilizing
276 reactive ABTS^{•-} radicals. The apparent improvement in
277 enzyme stability is tentatively attributed to the NPs, which
278 help prevent enzymes from interacting with each other without
279 significantly impeding enzyme diffusion.
280 In conclusion, this work demonstrates the ability of
281 polymeric glyconanoparticles containing redox-active bis-
282 pyrene-ABTS molecules to function as electron shuttles in
283 solution for the electrical wiring of BOx. Thanks to an intimate
284 MET exchange between nanoparticles containing a high density
285 of electron acceptors, enhanced catalytic currents have been
286 observed compared to homogeneous mediators. In addition to
287 enhanced catalytic performance and low overpotentials, the
288 biocathode with redox nanoparticles showed dramatically
289 improved stability after 60 min of operation and 24 h of
290 storage, suggesting that the polymer architecture stabilizes both
291 the enzyme and mediator. Furthermore, the large size of the
292 nanoparticles should permit their containment in permselective
293 membranes. In future work, the nanoparticle system will be
294 exploited to solubilize new hydrophobic mediators at high
295 concentrations for bioelectrocatalysis toward a refuelable all-in-
296 solution biofuel cell for powering electronics devices. Biofuel
297 cell designs are envisaged in which enzymes and nanoparticles
298 are periodically introduced to prolong biofuel cell lifetime.

299 ■ ASSOCIATED CONTENT

300 ● Supporting Information

301 The Supporting Information is available free of charge on the
302 ACS Publications website at DOI: 10.1021/jacs.7b09442.

303 Experimental details and characterization data (PDF)

304 ■ AUTHOR INFORMATION

305 Corresponding Authors

306 *borsali@cermav.cnrs.fr

307 *serge.cosnier@univ-grenoble-alpes.fr

308 ORCID

309 Andrew J. Gross: 0000-0002-7356-7089

310 Xiaohong Chen: 0000-0002-6535-3873

311 Fabien Giroud: 0000-0001-6611-2687

312 Redouane Borsali: 0000-0002-7245-586X

313 Notes

314 The authors declare no competing financial interest.

315 ■ ACKNOWLEDGMENTS

316 This work was supported by Labex Arcane (ANR-11-539-
317 LABX-0003-01), Nanobio Chimie ICMG FR2607 and Polynat
318 Carnot Institute. X. Chen is grateful for a Université Grenoble
319 Alpes Ph.D. scholarship. Dr. Eric Reynaud and Dr. Jean-Luc

Putaux are acknowledged for polymer synthesis and TEM
imaging, respectively.

■ REFERENCES

- (1) Moser, C. C.; Keske, J. M.; Warncke, K.; Farid, R. S.; Dutton, P. L. *Nature* **1992**, *355*, 796.
- (2) Saboe, P. O.; Conte, E.; Farrell, M.; Bazan, G. C.; Kumar, M. *Energy Environ. Sci.* **2017**, *10*, 14.
- (3) Cosnier, S.; Gross, A. J.; Le Goff, A.; Holzinger, M. *J. Power Sources* **2016**, *325*, 252.
- (4) Stines-Chaumeil, C.; Roussarie, E.; Mano, N. *Biochim. Open* **2017**, *4*, 36.
- (5) Tsujimura, S.; Tatsumi, H.; Ogawa, J.; Shimizu, S.; Kano, K.; Ikeda, T. *J. Electroanal. Chem.* **2001**, *496*, 69.
- (6) Kano, K.; Ikeda, T. *Anal. Sci.* **2000**, *16*, 1013.
- (7) Ruff, A. *Curr. Opin. Electrochem.* **2017**, just accepted, DOI: 10.1016/j.coelec.2017.06.007.
- (8) Xiao, Y.; Patolsky, F.; Katz, E.; Hainfeld, J. F.; Willner, I. *Science* **2003**, *299*, 1877.
- (9) Zayats, M.; Katz, E.; Baron, R.; Willner, I. *J. Am. Chem. Soc.* **2005**, *127*, 12400.
- (10) Lalaoui, N.; Rousselot-Pailley, P.; Robert, V.; Mekmouche, Y.; Villalonga, R.; Holzinger, M.; Cosnier, S.; Tron, T.; Le Goff, A. *ACS Catal.* **2016**, *6*, 1894.
- (11) Holland, J. T.; Lau, C.; Brozik, S.; Atanassov, P.; Banta, S. *J. Am. Chem. Soc.* **2011**, *133*, 19262.
- (12) Gutiérrez-Sánchez, C.; Pita, M.; Vaz-Domínguez, C.; Shleev, S.; De Lacey, A. L. *J. Am. Chem. Soc.* **2012**, *134*, 17212.
- (13) Trifonov, A.; Tel-Vered, R.; Fadeev, M.; Willner, I. *Adv. Energy Mater.* **2015**, *5*, 1401853.
- (14) Aquino Neto, S.; Forti, J. C.; Zucolotto, V.; Ciancaglini, P.; De Andrade, A. R. *Process Biochem.* **2011**, *46*, 2347.
- (15) Sheldon, R. A.; van Pelt, S. *Chem. Soc. Rev.* **2013**, *42*, 6223.
- (16) Li, J.-J.; Chen, Y.; Yu, J.; Cheng, N.; Liu, Y. *Adv. Mater.* **2017**, *29*, 1701905.
- (17) Gross, A. J.; Haddad, R.; Travelet, C.; Reynaud, E.; Audebert, P.; Borsali, R.; Cosnier, S. *Langmuir* **2016**, *32*, 11939.
- (18) Liu, P.; Sun, S.; Guo, X.; Yang, X.; Huang, J.; Wang, K.; Wang, Q.; Liu, J.; He, L. *Anal. Chem.* **2015**, *87*, 2665.
- (19) Mano, N.; Edembe, L. *Biosens. Bioelectron.* **2013**, *50*, 478.
- (20) Heller, A. *Phys. Chem. Chem. Phys.* **2004**, *6*, 209.
- (21) Goldsmith, J. I.; Takada, K.; Abruña, H. D. *J. Phys. Chem. B* **2002**, *106*, 8504.
- (22) Flexer, V.; Ielmini, M. V.; Calvo, E. J.; Bartlett, P. N. *Bioelectrochemistry* **2008**, *74*, 201.
- (23) Farneth, W. E.; Diner, B. A.; Gierke, T. D.; D'Amore, M. B. *J. Electroanal. Chem.* **2005**, *581*, 190.
- (24) Pankratov, D.; Sundberg, R.; Suyatin, D. B.; Sotres, J.; Barrantes, A.; Ruzgas, T.; Maximov, I.; Montelius, L.; Shleev, S. *RSC Adv.* **2014**, *4*, 38164.